

Global warming overshoots increase risk of triggering climate tipping points and cascades

Nico Wunderling (✉ nico.wunderling@pik-potsdam.de)

Potsdam Institute for Climate Impact Research <https://orcid.org/0000-0002-3566-323X>

Ricarda Winkelmann

Potsdam Institute for Climate Impact Research <https://orcid.org/0000-0003-1248-3217>

Johan Rockström

Potsdam Institute for Climate Impact Research

Sina Loriani

Potsdam Institute for Climate Impact Research

David Armstrong-McKay

Georesilience Analytics

Paul Ritchie

University of Exeter <https://orcid.org/0000-0002-7649-2991>

Boris Sakschewski

Potsdam Institute for Climate Impact Research

Jonathan Donges

Potsdam Institute for Climate Impact Research

Article

Keywords:

Posted Date: April 22nd, 2022

DOI: <https://doi.org/10.21203/rs.3.rs-1418830/v1>

License:  This work is licensed under a Creative Commons Attribution 4.0 International License.

[Read Full License](#)

1 Global warming overshoots increase risk of triggering
2 climate tipping points and cascades

3 Nico Wunderling,^{1,2,3*} Ricarda Winkelmann,^{1,4} Johan Rockström,^{1,2}
Sina Loriani,¹ David I. Armstrong McKay,^{5,6} Paul D.L. Ritchie,⁵
Boris Sakschewski,¹ and Jonathan F. Donges^{1,2,3*}

¹Potsdam Institute for Climate Impact Research (PIK), Member of the Leibniz Association,
14473 Potsdam, Germany

²Stockholm Resilience Centre, Stockholm University, Stockholm, SE-10691, Sweden

³High Meadows Environmental Institute, Princeton University, Princeton, 08544 New Jersey, USA

⁴Institute of Physics and Astronomy, University of Potsdam, 14476 Potsdam, Germany

⁵College of Engineering, Mathematics and Physical Sciences, University of Exeter,
Exeter, EX4 4QE, UK

⁶Georesilience Analytics, Leatherhead, UK

*Correspondences should be addressed to: nico.wunderling@pik-potsdam.de or jonathan.donges@pik-potsdam.de

4 **Climate tipping elements play a crucial role for the stability of the Earth sys-**
5 **tem under human pressures and are potentially at risk of disintegrating within**
6 **and partially even below the Paris temperature guardrails of 1.5–2.0°C above**
7 **pre-industrial levels. However, current policies and actions make it very likely**
8 **to, at least temporarily, transgress the Paris targets. This raises the question**
9 **whether tipping points can still be avoided under such overshoot scenarios.**
10 **Here, we investigate the associated risks for tipping under a range of temper-**
11 **ature overshoot scenarios using a stylised network model of four interacting**
12 **climate tipping elements: the Greenland and West Antarctic Ice Sheets, the**
13 **Atlantic Meridional Overturning Circulation and the Amazon rainforest. Our**
14 **results reveal that temporary overshoots can increase tipping risks by up to**
15 **72% compared to a soft landing without overshoots, even when the long-term**
16 **equilibrium temperature stabilises within the Paris range. Moreover, we find**
17 **that modest interaction strength levels between the tipping elements are re-**
18 **sponsible for 49% more tipped elements than without cascading interactions.**
19 **Our analysis shows that avoiding a *high climate risk zone*, which minimise**
20 **risks for triggering tipping dynamics requires both long-term temperatures**
21 **to stabilise at or below today’s levels of global warming, and low temperature**
22 **overshoots at the same time.**

23 It has long been proposed that important continental-scale subsystems of the Earth's climate
24 system possess nonlinear behaviour^{1,2}. The defining property of these tipping elements are
25 their self-perpetuating feedbacks once a critical threshold is approached or transgressed³ such
26 as the melt-elevation feedback for the Greenland Ice Sheet⁴ or the moisture recycling feedback
27 for the Amazon rainforest⁵. Global mean surface temperature has been identified as the driving
28 parameter for the state of the climate tipping elements^{1,6,7}, which include, among others, sys-
29 tems like the large ice sheets on Greenland and Antarctica, the Atlantic Meridional Overturning
30 Circulation (AMOC), or the Amazon rainforest^{8,9,10,11}.

31 Besides further amplifying global warming³, the disintegration of such climate tipping elements
32 individually would have large consequences for the biosphere and human civilisations, includ-
33 ing sea-level rise over very long time periods, large-scale biome shifts and collapses, or shifts
34 of monsoon systems. Since the first mapping of climate tipping elements in 2008¹ the scientific
35 focus has increased, with a 2019 warning that nine of the known 15 climate tipping elements
36 are showing signs of instability¹², followed by a listing of all known climate tipping elements
37 with levels of tipping point likelihoods in the IPCC AR6¹³. As this science has advanced tem-
38 perature thresholds have been corrected downwards several times¹². The most recent scientific
39 assessment places the critical threshold temperatures of triggering tipping points at 1–5°C, with
40 moderate risks already at 1.5–2°C for several systems, like the Greenland and the West Antarctic
41 Ice Sheets⁶. In this sense, tipping elements research provides even further scientific support to
42 hold global mean surface temperatures within the Paris range of 1.5–2°C, while at the same time
43 emphasising the tipping point risks cannot be ruled out even at this lower temperature range⁷.

44 There is thus a triple dilemma emerging here. First, insufficient policies and actions means
45 that the world is following a trajectory well-beyond 2°C by the end of this century¹⁴. Second,
46 essentially all IPCC scenarios that hold the 1.5°C line include a period of several decades of
47 temperature overshoot¹³. And third, given that tipping elements research can no longer exclude

48 crossing tipping points already at low temperature ranges ($<2^{\circ}\text{C}$), more knowledge is urgently
49 needed on risks of crossing tipping points during periods of overshoot^{15,16,17}.
50 Therefore, it is essential to assess the temperature overshoots and long-term temperature stabil-
51 isations that can lead to irreversible changes in the climate system. While the impacts of over-
52 shoots have been investigated from a mathematical point of view and a climate tipping element
53 view for individual elements^{15,18,19}, climate tipping elements interact across scales in space and
54 time, creating risks of additional feedback dynamics^{12,20,21,22}. Interactions may increase tipping
55 risks by triggering cascades, when tipping of one element triggers tipping of connected tipping
56 elements²³. Therefore in this work, we combine the research on interactions between climate
57 tipping elements and temperature overshoots. In this study, we systematically assess the risk
58 for tipping and identify a high climate risk zone, considering remaining uncertainties in the
59 properties of the tipping elements and different global warming overshoot scenarios if Paris
60 temperature targets are not met without overshoots.

61

62 **Simulation procedure of overshoots applied to tipping elements**

63 Following Wunderling et al. (2021)²³, we use a stylised network model of ordinary differential
64 equations designed for risks analysis to couple four climate tipping elements (see Methods):
65 the Greenland Ice Sheet, the West Antarctic Ice Sheet, the AMOC, and the Amazon rainforest
66 (see map in Fig. 1). In this model, the interactions between these tipping elements and the
67 driving physical mechanisms are estimated on a formalised expert elicitation²², enabling to
68 assess cascading tipping risks at a certain level of global warming. Our network model is
69 able to capture the main dynamics of these interacting tipping elements, and is therefore able to
70 propagate important uncertainties in the input parameters. These include the critical temperature
71 thresholds and the typical tipping time scales of the individual tipping elements, as well as the
72 interaction strengths and interaction network structure. The low computational complexity of

73 our approach allows to sample this parameter space by means of a very large-scale Monte
74 Carlo ensemble simulation, including approximately 3.8 million individual ensemble members
75 (model simulation runs) in total. For the construction of the ensemble, but also for the boundary
76 values of the parameters uncertainties (based on the latest literature review⁶), see Methods.
77 In these numerical experiments, the four tipping element network is exposed to different global
78 warming overshoot scenarios characterised by the peak temperature, duration of the overshoot,
79 and the final convergence temperature reached in long-term equilibrium (see Fig. 1a). All these
80 are important properties of the overshoot trajectory in determining the outcome of a poten-
81 tial tipping event. The stylised temperature overshoot trajectories applied to the four inter-
82 acting climate tipping elements, were primarily designed to capture typical temperature pro-
83 files generated by Earth System Model simulations for low to medium emissions scenario²⁴.
84 Moreover, the formulation of the trajectories allows for flexibility in how society manages the
85 transition from current warming to the convergence temperature, which can therefore lead to
86 overshoot trajectories¹⁵. To this end, our ensemble spans all combinations of (i) peak temper-
87 atures $T_{\text{Peak}} = 2.0, 2.5, \dots, 6.0^\circ\text{C}$ (maximally reached temperature), (ii) convergence tempera-
88 tures $T_{\text{Conv}} = 0.0, 0.5, \dots, 2.0^\circ\text{C}$ (final stabilisation temperature), and (iii) convergence times
89 $t_{\text{Conv}} = 100, 200, \dots, 1000$ years (time to reach T_{Conv}), allowing us to quantify the respective
90 risk and time scale for tipping events. Not that the limit case of $T_{\text{Peak}} = T_{\text{Conv}} = 2.0^\circ\text{C}$ is
91 simulated as constant temperature. In this paper, we will focus on peak temperatures up to
92 4.0°C , where 4.0°C represents an upper temperature limit we investigate, based on *policies and*
93 *targets* following COP26 and the climate-action-tracker¹⁴. High-end warming scenarios with
94 peak temperatures of $4.5\text{--}6.0^\circ\text{C}$ are added in the supplementary material, which allow com-
95 puting a comprehensive risk analysis. Fig. 1a presents an exemplary timeline of an overshoot
96 trajectory that peaks at 2.5°C warming and converges to a 2.0°C convergence temperature after
97 400 years. The impact on the four studied interacting tipping elements is shown in Fig. 1b.

98 For this scenario, the global mean temperature (GMT) remains above the critical threshold of
99 the Greenland Ice Sheet and therefore causes tipping. However, the Greenland Ice Sheet has
100 a slow tipping time scale, while the melting trajectory is irreversible, taking over 1,000 years
101 to transition to an ice-free state. Despite GMT briefly exceeding the AMOC critical threshold,
102 this is not enough to cause the AMOC to tip initially. However, the Greenland Ice Sheet tipping
103 causes the AMOC to tip later (on a faster timescale of roughly 100 years) due to the strong
104 coupling between the two elements. Additionally in this scenario, the West Antarctic Ice Sheet
105 tips as a result of both the Greenland Ice Sheet and the AMOC tipping. The tipping time scale
106 of the West Antarctic Ice Sheet is slow and so with the Greenland Ice Sheet as the initiator, the
107 overall tipping of the three elements takes 1,000 years to complete. Some further exemplary
108 scenarios are provided in supp. Fig. S1. In the remainder of this work, the impact of a certain
109 relevant parameter combination ($T_{\text{Peak}}, T_{\text{Conv}}, t_{\text{Conv}}$) on the risk of an element tipping is given by
110 the fraction of all simulation runs that result in a tipped state, averaged over all other parame-
111 ters and uncertainties. In this study, we define the tipping of an element as the tipping process
112 being completed, i.e. when the tipping element reaches the transitioned regime (cf. Fig. 1b).
113 In the remainder of this work, we first evaluate the tipping risk with respect to the overshoot
114 peak temperature, convergence temperature and convergence time, and identify risk maps for a
115 high climate risk zone. Second, we determine the mechanisms for tipping events and, third, we
116 investigate the role of interactions and quantify the amount and share of tipping cascades.

117

118 **The effects of overshoot peak temperature**

119 Focusing on the role of overshoot peak temperature, we find that the risk for the emergence of
120 at least one tipping event increases with rising peak temperature. Averaged over all ensemble
121 members, around one-third ($36.5 \pm 5.0\%$) of all simulations show a tipping event or cascade at a
122 peak temperature of 2.0°C above pre-industrial, while it is close to three-quarters ($74.3 \pm 1.4\%$)

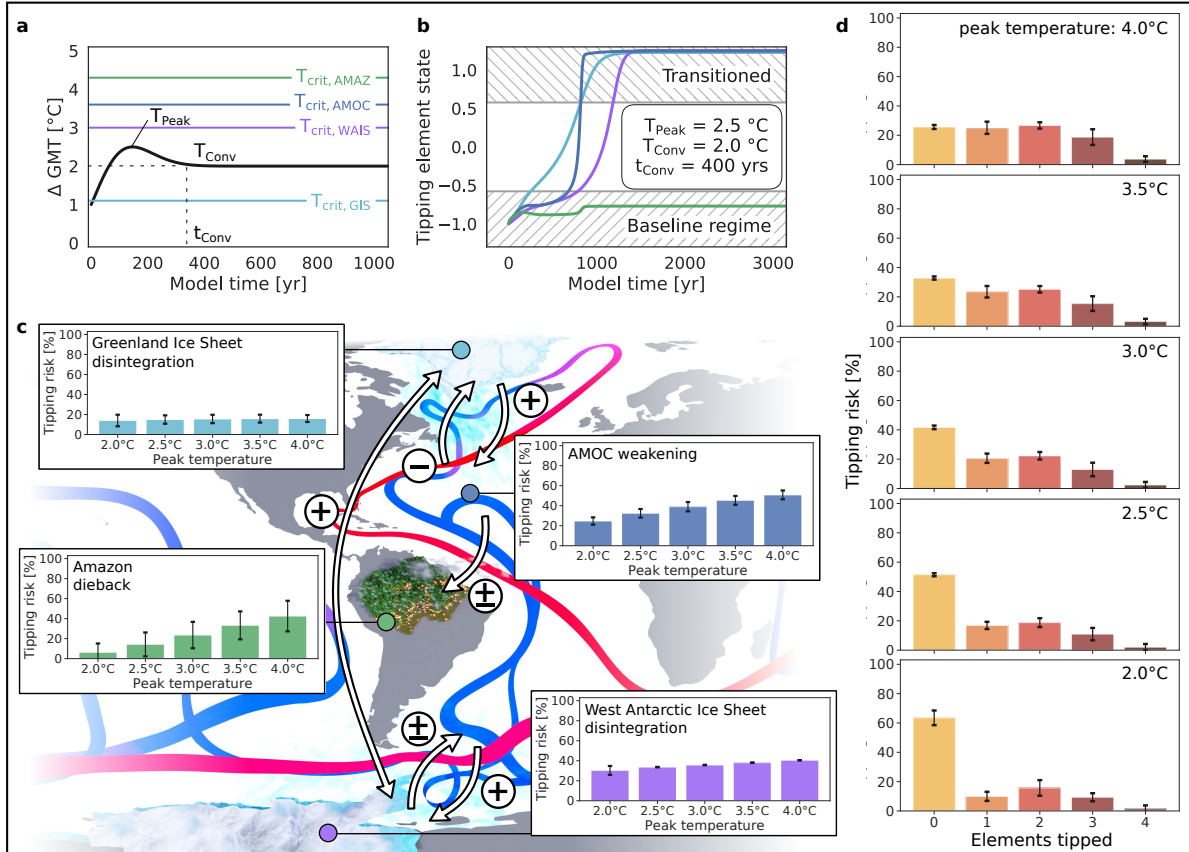


Figure 1 | Effect of overshoots on interacting climate tipping elements. **a**, Exemplary global warming overshoot scenario with a peak temperature of $T_{\text{Peak}} = 2.5^{\circ}\text{C}$, a convergence temperature of $T_{\text{Conv}} = 2.0^{\circ}\text{C}$ above pre-industrial, and a time to convergence to 2.0°C of $t_{\text{Conv}} = 400$ years. This scenario is applied to a set of four investigated interacting climate tipping elements. **b**, The effect of the overshoot trajectory shown in panel a: the Greenland Ice Sheet, the West Antarctic Ice Sheet and the AMOC tip. For further exemplary overshoot scenarios and the exact parameter values, see supp. Fig. S1. **c**, Map of four interacting climate tipping elements: Greenland Ice Sheet, West Antarctic Ice Sheet, AMOC and Amazon rainforest. The insets show the individual risk of transitioning into the undesired state in dependence of overshoot peak temperatures of 2.0 – 4.0°C above pre-industrial levels. **d**, Number of tipped elements in dependence of overshoot peak temperatures of 2.0 – 4.0°C above pre-industrial. The errors depict the standard deviation considering uncertainties in the interaction network structure. High-end overshoot peak temperatures up to 6.0°C above pre-industrial levels and tipping times (after 100 yrs, 1,000 yrs, and in equilibrium), are shown in supp. Fig. S2.

123 of all simulations at 4.0°C peak temperature (Fig. 1d). However, the dependence on the peak
124 temperature is unevenly distributed among the four different climate tipping elements (see in-
125 sets in Fig. 1c). The tipping risk for tipping elements with high inertia (slow tipping elements:
126 Greenland and West Antarctic Ice Sheets) remains constant over an increasing peak tempera-
127 ture because their reaction time (500-13,000 years) is slow against the duration of the overshoot
128 trajectory ($t_{\text{Conv}} = 100 - 1,000$ years). Therefore, e.g., the tipping risk for the Greenland
129 Ice Sheet remains relatively constant between $T_{\text{Peak}} = 2.0^\circ\text{C}$ (tipping risk: $14.0 \pm 5.7\%$) and
130 $T_{\text{Peak}} = 4.0^\circ\text{C}$ (tipping risk: $16.0 \pm 3.5\%$, see insets in Fig. 1c). In contrast, for tipping elements
131 with low inertia (fast tipping elements: AMOC and Amazon rainforest) there is a strong tipping
132 risk increase, comparing scenarios of $T_{\text{Peak}} = 2.0^\circ\text{C}$ (tipping risk of AMOC: $24.7 \pm 3.7\%$) with
133 $T_{\text{Peak}} = 4.0^\circ\text{C}$ (tipping risk of AMOC: $50.8 \pm 4.4\%$, see insets in Fig. 1c). On the other hand, the
134 tipping risk for the slow tipping elements increases for increasing convergence times (see supp.
135 Fig. S3), whereas the tipping risk for the fast tipping elements only increases slightly for in-
136 creasing convergence times above 200 years. This subsequent increase can largely be attributed
137 to cascading effects, where typically the Greenland Ice Sheet tipping has initiated tipping on
138 the faster elements. For peak temperatures above 5.5°C, it becomes highly likely (virtually cer-
139 tain, i.e. >95%) that at least one tipping element transitions to its alternative state (see supp.
140 Fig. S2). Fig. 1 shows the equilibrium results after 50,000 simulation years, which demon-
141 strate the long-term commitment due to transgressed tipping thresholds. While this provides
142 an important insight into potential locked-in change, some tipping risks are already realised
143 after 100–1,000 years. On these shorter time scales, especially the AMOC and the Amazon
144 rainforest show a strong dependence on the peak temperature (see supp. Fig. S2). Especially
145 for the West Antarctic Ice Sheet, new literature results suggest lower temperature thresholds as
146 before^{6,7}. Therefore, considerable tipping risks ($30.3 \pm 4.5\%$) can be observed already at peak
147 temperatures of 2.0°C (see Fig. 1c insets).

148

149 **Risk maps for identifying a high climate risk zone**

150 For final convergence temperatures comparable with today's levels of warming (approx. $T_{\text{Conv}} =$
151 1.0°C), we find that the expected number of tipped elements is at least $\langle \# \rangle_{\text{tipped,min}} = 0.29$
152 (see Fig. 2). This minimal number of tipped elements is evaluated for the most optimistic case
153 of this study (lowest-left parameter combination in Fig. 2a, b, c), where the peak temperature
154 reaches 2.0°C above pre-industrial and the convergence time to the final temperature is 100
155 years. The tipping risk that at least one tipping element transitions to its alternative state (related
156 to $\langle \# \rangle_{\text{tipped,min}} = 0.29$) is 15%, see Fig. 2d. Stabilising global warming at the lower limit of
157 the Paris range at 1.5°C above pre-industrial levels, increases the number of minimally tipped
158 elements to 1.19, and for a stabilisation at the upper Paris limit of 2.0°C , we find at least 1.89
159 tipped elements on average (compare Fig. 2a, b, c).

160 Going from the number of tipped elements to tipping risks, we define a *high climate risk zone*
161 as the region, within which the likelihood for no tipping event to occur is larger than 66%, or
162 the risk that one or more elements tip is lower than 33%. We compute this risk and find an
163 increase from 15% over 56% to 82% at convergence temperatures of 1.0, 1.5 and 2.0°C for
164 the most optimistic parameters ($t_{\text{Conv}} = 100$ years and $T_{\text{Peak}} = 2.0^{\circ}\text{C}$, compare Fig. 2d, e, f).
165 These results lead to the conclusion that the high climate risk zone spans the entire state space
166 for final convergence temperatures of $1.5\text{--}2.0^{\circ}\text{C}$. Only if final convergence temperatures are
167 limited to, or better below, today's levels of global warming, while peak temperatures are below
168 3.0°C , the tipping risks remain below 33% (see Fig. 2d). In parallel, the equipotential lines shift
169 strongly from higher peak temperatures and convergence times to lower ones with increasing
170 convergence temperature. This leads to a lower likelihood of low-risk scenarios without tipping
171 elements transitioning to their alternative state. In the worst case of a convergence temperature
172 of 2.0°C (see Fig. 2f), the tipping risk for at least one tipping event to occur is on the order of

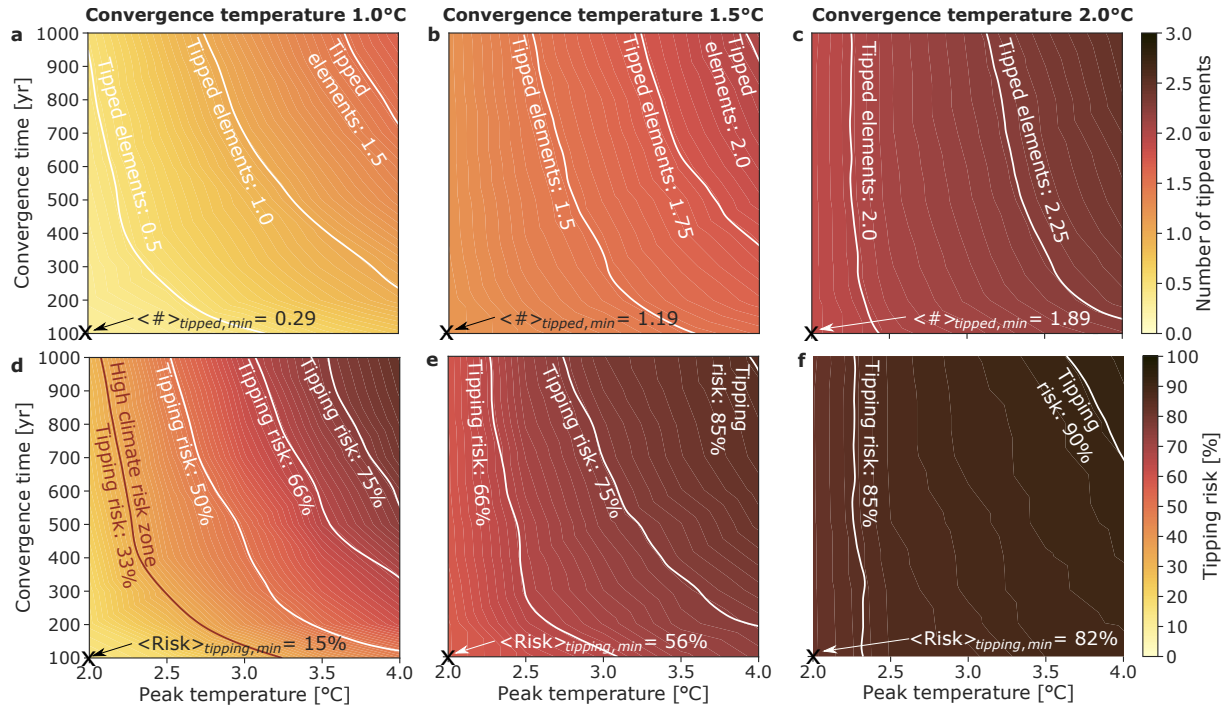


Figure 2 | Expected number and risk of tipping events at different convergence temperatures. **a**, Number of tipped elements averaged over the entire ensemble for all investigated convergence times $t_{\text{Conv}} = 100, 200, \dots, 1000$ years and peak temperatures $T_{\text{Peak}} = 2.0, 2.5, \dots, 4.0^\circ\text{C}$ at a convergence temperature of $T_{\text{Conv}} = 1.0^\circ\text{C}$ above pre-industrial levels. The white lines show the conditions at which 0.5, 1.0, and 1.5 elements are tipped on average. $\langle \# \rangle_{\text{tipped, min}}$ is the average number of tipped elements at $t_{\text{Conv}} = 100$ years and $T_{\text{Peak}} = 2.0^\circ\text{C}$, which is the most optimistic case. **b**, **c**, Same as in **a**, but for convergence temperatures of 1.5°C and 2.0°C , respectively. Note that the white equipotential lines denote 1.5, 1.75 and 2.0 tipped elements in panel **b**, and 2.0 and 2.25 tipped elements in panel **c**. **d**, The risk that at least one tipping element transitions to its alternative state at the end of the simulation (after 50,000 simulation years, equilibrium simulation) for a convergence temperature of 1.0°C . The equipotential line in red indicates the *high climate risk zone* (tipping risk is equal to 33%), while the further white lines indicate risks of 50%, 66% and 75%, respectively. $\langle \text{Risk} \rangle_{\text{tipping, min}}$ is the average risk of at least one element being tipped at $t_{\text{Conv}} = 100$ years and $T_{\text{Peak}} = 2.0^\circ\text{C}$. **e**, **f**, Same as for **d**, but for convergence temperatures of 1.5°C and 2.0°C , respectively. Note that the equipotential lines indicate 66%, 75% and 85% (panel **e**), and 85% and 90% (panel **f**) that at least one element is tipped. The simulations for $T_{\text{Conv}} = 0.0^\circ\text{C}$ (return to pre-industrial temperatures) and $T_{\text{Conv}} = 0.5^\circ\text{C}$ can be found in supp. Fig. S4. High-end scenarios with $T_{\text{Peak}} = 4.0\text{--}6.0^\circ\text{C}$ are added in supp. Figs. S5 and S6.

173 above 90% if peak temperatures of 4.0°C are not prevented. So, considering all the uncertainties
174 in the ensemble, only less than 10% of the ensemble members remain free of tipping events
175 in this case. The devastating negative consequences of such a scenario with high likelihood
176 of triggering tipping events would entail significant sea level rise, biosphere degradation or
177 considerable North Atlantic temperature drops.

178 Therefore, this would entail an *unsafe overshoot* regime. On the other hand, strictly lowering
179 the final convergence temperature of or below today’s levels of global warming while limiting
180 peak overshoot temperatures to 3.0°C and convergence times in parallel significantly reduces
181 the risk of tipping events (see Fig. S4 and Fig. 2d). In the most optimistic scenario, tipping risks
182 are kept below 5%.

183

184 **Tipping mechanisms and timing under current climate trajectories**

185 The risk for tipping events increases with higher peak temperatures, higher convergence temper-
186 atures, and longer convergence times. However, the mechanism causing a tipping event to occur
187 in our model is twofold: (i) The element tips due to the final temperature T_{Conv} being higher than
188 its critical temperature threshold. We call this *baseline tipping* because the final baseline, i.e.
189 the convergence temperature, is already higher than the critical temperature. An example for
190 baseline tipping for the Greenland Ice Sheet can be found in Fig. 1a, b. (ii) The element tips due
191 to the temperature overshoot trajectory, which temporarily transgresses its critical temperature
192 threshold. We call this *overshoot tipping*. In both cases, baseline tipping or overshoot tipping,
193 the first tipped element can draw along other elements in a tipping cascade such that the size
194 of the cascade is not necessarily restricted to one. We compute that the risk for tipping events
195 occurring at convergence temperatures within the limits of the Paris climate target ranges be-
196 tween slightly more than half (57.8%) to more than nine-tenths (91.4%) of all simulations (see
197 Fig. 3). For small peak temperatures ($T_{\text{Peak}} = 2.5^\circ\text{C}$), overshoot tipping only accounts for as

198 little as 9% of all tipping events but for intermediate peak temperature levels ($T_{\text{Peak}} = 4.0^{\circ}\text{C}$)
199 this number can increase to as much as 42% (see pie charts in Fig. 3). Specifically, the risk of
200 tipping increases between 10–72% in these scenarios for overshooting before stabilising at the
201 convergence temperature than just approaching the convergence temperature with no overshoot.
202 Note that in the special case, where the peak temperature equals the convergence temperature
203 ($T_{\text{Peak}} = T_{\text{Conv}} = 2.0^{\circ}\text{C}$), overshoot tipping events do not occur.

204 The number of expected tipping events increases from short to long time scales as tested in our
205 experiments, where we separated tipping events realised after 100 (short-term tipping), 1,000
206 (mid-term tipping) and 50,000 simulation years (equilibrium tipping, see bar charts in Fig. 3).
207 For higher peak temperatures, we additionally observe a larger portion of tipping events realised
208 within 100 and 1,000 years. These short-term events are dominantly caused by the fast tipping
209 elements (AMOC and Amazon rainforest), but mid-term events are additionally also partially
210 caused by a tipping West Antarctic Ice Sheet (see supp. Fig. S2). Together our results indicate
211 that in order to avoid tipping events within the Paris range, not only the peak temperature must
212 be limited but also the final convergence temperature must fall significantly below 1.5°C in the
213 long run. This would reduce the tipping risk to 8.8–23.4% if final convergences temperatures
214 range between $0.0\text{--}1.0^{\circ}\text{C}$ and $T_{\text{Peak}} = 2.0^{\circ}\text{C}$ (see supp. Fig. S7). To further hedge these tipping
215 risks, the time to reach the convergence temperature must also be small (i.e. $t_{\text{Conv}} \lesssim 200$ yrs,
216 cf. supp. Fig. S4c,d). However, current *policies and action* would lead to $2.0\text{--}3.6^{\circ}\text{C}$ (mean:
217 2.7°C), and present *pledges and targets* to $1.7\text{--}2.6^{\circ}\text{C}$ (mean: 2.1°C) above pre-industrial, based
218 on the COP26-update published in November 2021 (see climateactiontracker and vertical axis
219 in Fig. 3c)¹⁴ as expected temperatures in 2100. As noted above, these temperatures would
220 lead to significant tipping risks if they were interpreted as peak temperatures. If they would
221 be convergence temperatures, tipping very likely is unavoidable. Additionally, high-end sce-
222 nario simulations with very high peak temperatures between $4.5\text{--}6.0^{\circ}\text{C}$ reveal that the risk to

223 observe tipping becomes virtually certain ($>95\%$ for $T_{\text{Peak}} \gtrsim 5.5^\circ\text{C}$). At these scenarios, it is
 224 likely ($>40\%$) that the first tipping event would occur within 100 years, typically the Amazon
 225 rainforest or the AMOC (see supp. Fig. S8).

226

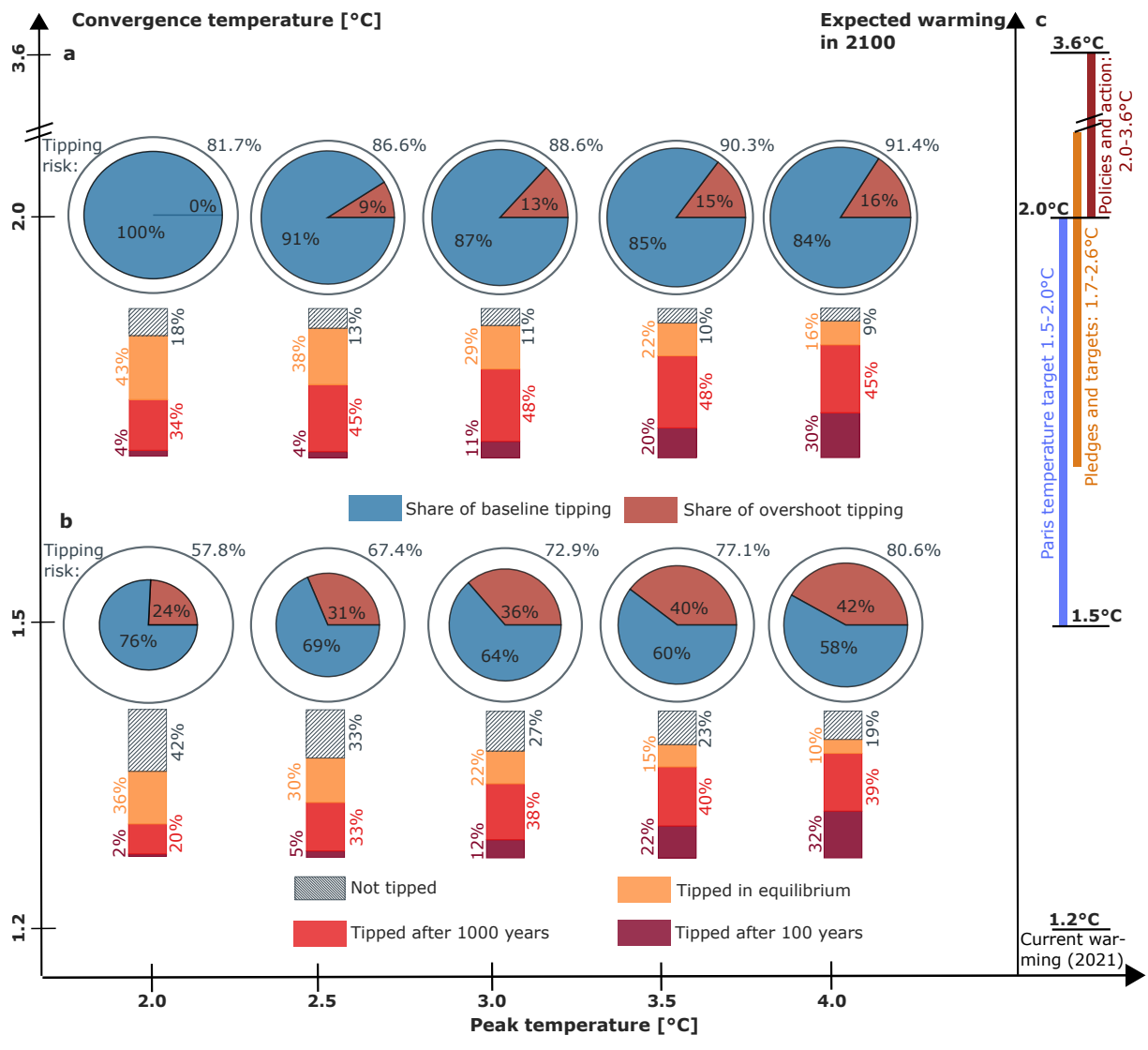


Figure 3 | Mechanisms and timing of tipping events following a temperature overshoot.

Here, we show the risk for tipping with respect to overshoot scenarios of 2.0–4.0°C and convergence temperatures within the Paris range of 1.5–2.0°C above pre-industrial. The size of the *pie-chart* indicates the overall tipping risk (e.g. 67.4% at $T_{\text{Conv}}=1.5^\circ\text{C}$ and $T_{\text{Peak}}=2.5^\circ\text{C}$). The number of observed tipping events can be separated into two mechanisms: (i) due to the convergence temperature being above the critical temperature for one or several tipping elements (*baseline tipping*, example see Greenland Ice Sheet in Fig. S1d, e), and (ii) due to the overshoot trajectory (*overshoot tipping*, example see AMOC in Fig. S1c). The *bar chart* directly below the pie-chart splits the tipping events into the time-scale when they occur. Either after 100 simulation years (dark red), 1,000 simulation years (light red), in equilibrium simulations (after 50,000 simulation years, orange), or not at all (hatched). **a**, Scenario where global mean temperature converges to 1.5°C. **b**, Scenario where global mean temperature converges to 2.0°C. **c**, Expected warming in 2100 after the COP26 *pledges and targets* (orange vertical line: 1.7–2.6°C), and the *policies and action* (dark red vertical line: 2.0–3.6°C) together with the current warming of 1.2°C and the Paris temperature target (blue vertical line: 1.5–2.0°C). Note that the vertical axes are nonlinear due to visibility. The data for the vertical lines has been compiled from the November 2021 update by climateactiontracker¹⁴. The scenarios with lower convergence temperatures of 0.0, 0.5, and 1.0°C above pre-industrial are depicted in supp. Fig. S7. High-end climate scenarios and overshoots for peak temperatures between 4.5–6.0°C are shown in supp. Fig. S8.

227 The role of interactions and cascading effects

228 An interesting aspect, which has not been investigated before, are the effects of interactions
229 on the risk of (cascading) transitions in overshoot scenarios. The average number of tipped
230 elements increases with increasing interaction strength (see Fig. 4). Here, an interaction
231 strength of 0.0 represents four individual uncoupled tipping elements, while an interaction
232 strength of 1.0 represents the case where the interactions are approximately as important as the
233 individual dynamics²³. For convergence temperatures of 1.5 or 2.0°C, we find a notable effect
234 of increasing number of tipped elements due to cascading interactions between interaction
235 strength values of 0.0–0.3. The total effect at a convergence temperature of 1.5°C increases
236 the average tipped number from 1.04 ± 0.04 at an interaction strength of 0.0 to 1.46 ± 0.03 at

237 an interaction strength of 0.3, corresponding to an increase of $40.4 \pm 3.9\%$. For a convergence
238 temperature of 2.0°C , the increase of the average number of tipped elements makes up an
239 additional $49.3 \pm 2.1\%$. In this case, a further increase of the interaction strength from 0.3 to 1.0,
240 only leads to a marginal additional tipping risk of $12.1 \pm 0.5\%$. The reason for this nonlinear
241 increase in tipping at low to moderate interaction strength levels are cascading transitions
242 because higher convergence temperatures cause more tipping cascades than lower convergence
243 temperatures (compare Fig. 4a with Fig. 4b, c). This effect is most clearly apparent in the
244 equilibrium effects over a long time scale (orange bars), while time scales up to 1,000 years
245 show a relatively linear increase of tipped elements with increasing interaction strength (red
246 bars), and in contrast to a nearly constant number of tipped elements for time scales up to
247 100 years (dark red bars). This implies that the interactions between climate tipping elements
248 require a significant amount of time for their effect to be observable in the number of tipped
249 elements. This can be explained by the roles of the tipping elements in cascading transitions. It
250 has been found in earlier research that the slow tipping elements (Greenland and West Antarctic
251 Ice Sheet) are the main initiators of cascading transitions²³, but they also need the largest
252 amount of time to commence a transition, the effects of which can then be transported to further
253 tipping elements (AMOC and Amazon rainforest) via the respective physical interactions.
254 Therefore, the role of interactions, and with that the amount of tipping cascades, can most
255 clearly been seen for the long-term equilibrium experiments (see orange bars in Fig. 4). Lastly,
256 it is notable that the proportion of equilibrium tipping events goes down with decreasing
257 convergence temperature (see Fig. 4). For convergence temperatures of 0.0, 0.5, and 1.0°C
258 above pre-industrial levels, elements tipped in equilibrium do not play a role because in these
259 latter scenarios the number of baseline tipping scenarios is insignificantly small and overshoot
260 tipping does only rarely occur for the slow tipping elements (see supp. Fig. S9).

261

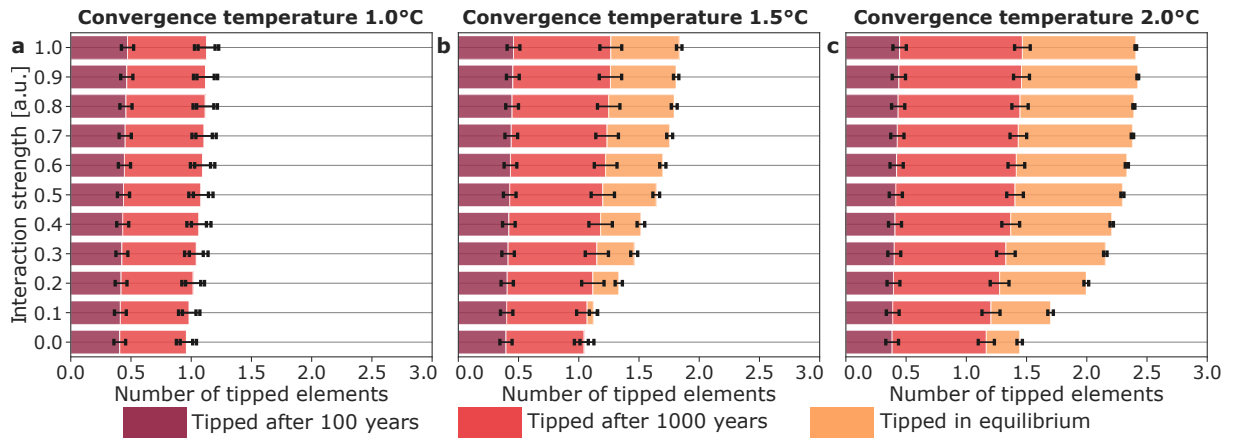


Figure 4 | Effect of interaction strength between climate tipping elements. Number of tipped elements against the interaction strength, separated into the respective tipping times (dark red: tipped after 100 simulation years, red: tipped after 1,000 simulation years, orange: tipped in equilibrium after simulation 50,000 years) for a convergence temperature of **a**, 1.0°C, **b**, 1.5°C and **c**, 2.0°C above pre-industrial levels. The errors show the standard deviation over the different interaction network realisations. For convergence temperatures of 0.0°C and 0.5°C above pre-industrial levels, see supp. Fig. S9.

Discussion

In summary, we find that the high climate risk zone characterised by large tipping risks (>33%) can only be avoided if several aspects are met in parallel due to the different time scales involved. These aspects are limited overshoot peak temperatures, limited convergence times, and most importantly limited convergence temperatures (due to baseline tipping) to levels at, or better, below the current level of global warming (1.2°C)¹⁴. Our analysis shows that the overshoot peak temperature should be constrained based on fast tipping elements (see Fig. 1c), whereas slow tipping elements largely determine the upper limit for convergence times (see supp. Fig. S3). The convergence temperature needs to be limited to avoid baseline tipping, and lower levels of it will also assist in avoiding overshoot tipping (see Fig. 3). Therefore, the combination of the slow Greenland Ice Sheet having a low temperature threshold and the faster elements (AMOC, Amazon rainforest) having at least partially higher thresholds (see supp. Tab. S1), facilitates the possibility of a small overshoot without causing tipping events and thus

275 further cascades. Ritchie et al. (2021)¹⁵ came to similar conclusions for individual tipping
276 elements but we find, for a sufficient interaction strength, a marked increase in the expected
277 number of tipped elements in equilibrium due to the possibility of emerging tipping cascades
278 (see Fig. 4). Taken together, safe and unsafe temporary overshoot trajectories can clearly be
279 separated.

280 Our employed stylised network model does not directly capture physical processes in its differ-
281 ential equations, and can as such not be used as a model for predictions, but has been designed
282 as a risk assessment tool for some of the most nonlinear entities in the Earth system. The
283 choices of our stylised global warming overshoot scenarios are motivated by current knowl-
284 edge, summarising short and long-term effects. The shape of the short-term overshoot trajec-
285 tories captures the temperature profiles from different Earth system model simulations²⁴, but is
286 still of conceptualised nature (see Eq. 2). To allow for a direct comparison to the baseline criti-
287 cal temperatures, we keep the temperature trajectories at constant levels in the long run. While
288 this is supported by ZECMIP (Zero Emissions Commitment Model Intercomparison Project)
289 for the near- to intermediate future for decades to centuries^{25,26}, it is unclear how carbon sinks
290 and sources behave for the more distant future. On time scales of centuries to millennia, it
291 seems more likely than not that a slight downward trend of global mean temperatures will be
292 entered^{26,27,28}. Still, large uncertainties remain and make future research necessary as has for
293 instance been proposed by using a novel framework of model experiments for zero emission
294 simulations²⁹. Overall, it is questionable whether this effect of naturally decreasing tempera-
295 tures would be sufficient to bring global mean temperatures after an overshoot back down to
296 safe levels without additional artificial carbon removal from the atmosphere²⁸.

297 A benefit of low complexity models such as ours is that they allow for very large-scale Monte
298 Carlo ensemble simulations, which can take into account relevant uncertainties such as in inter-
299 action structure, strength and critical temperature thresholds. One prominent example, which

300 we consider in our Monte Carlo ensemble, is the uncertainty on the interaction of the AMOC
301 with the Amazon rainforest, which could either be negative, positive or zero²², leading to rel-
302 atively large tipping risk errors for the Amazon rainforest (see insets of Fig. 1c). In principle,
303 our model is also flexible enough such that new tipping elements and their interaction structure
304 can be added, or it can be easily re-run to include updated knowledge on the tipping elements, if
305 necessary. Still, it should be aimed at building more complex models around coupled nonlinear
306 phenomena and climate tipping elements, either by combining simple physics-based models and
307 combining those models with observational data^{30,31,32}, or by employing Earth System Models
308 of either intermediate or high complexity. In the latter case, tipping elements could be spatially
309 resolved, which might refine or modify some of the results gained here³³. Moreover, data-
310 based approaches should be considered, with which it might be possible to reconstruct actual
311 interaction strength values. This might be possible using machine learning techniques based
312 on remote sensing data or, potentially, could be similar to already available investigations on
313 nonlinear changes in the Earth system^{34,35}. Recently, it has also been proposed to combine these
314 two research strands, with data-based approaches making use of artificial intelligence and Earth
315 system modelling, to create “neural” Earth system models³⁶.

316 Critically, to reduce the risk and prevent the negative impacts of interacting climate tipping el-
317 ements on human societies and biosphere integrity, it is of utmost importance to ensure that
318 temperature overshoot trajectories are limited in both magnitude and duration, while stabilising
319 global warming at, or better, below the Paris agreement’s targets. Concretely, avoiding a high
320 climate risk zone aiming to limit the risk for tipping events would entail convergence tempera-
321 tures of today’s levels of global warming or below ($< 1.2^{\circ}\text{C}$, better $\lesssim 1.0^{\circ}\text{C}$), while overshoot
322 temperatures should not exceed 3.0°C and convergence times should not exceed 300 years un-
323 less peak temperatures are significantly smaller than 2.5°C . This would reduce the risk for one
324 tipping event to occur to below 33% (see Fig. 2d). Although our results motivate that a future

325 climate trajectory without or with limited temperature overshoots would be preferable, current
326 results from the COP conferences and their pledges and targets indicate that at least temporary
327 overshoots over the Paris range seems likely^{14,37}. This would not only be problematic because
328 of natural risks exerted by disintegrated climate tipping elements, but also economic damages
329 would be smaller in case of a no-overshoot scenario, as has been shown in recent literature^{37,38}.
330 Even without overshoots though, economic damages could be tremendous due to the irreversible
331 nature of climate tipping elements and their interactions^{39,40,41}.

332 **Methods**

333 **Interacting climate tipping element model.** We use the stylised network model designed for
334 risk analysis of four interacting tipping elements detailed in Wunderling et al. (2021)²³. Each
335 tipping element is described by the following differential equation

$$\frac{dx_i}{dt} = \left[-x_i^3 + x_i + \sqrt{\frac{4}{27}} \cdot \frac{\Delta\text{GMT}(t)}{T_{\text{crit},i}} + d \cdot \sum_{\substack{j \\ j \neq i}} \frac{s_{ij}}{10} (x_j + 1) \right] \frac{1}{\tau_i}. \quad (1)$$

336 Here, x_i describes the state of the respective tipping element $i = \text{GIS}, \text{AMOC}, \text{WAIS}, \text{AMAZ}$
337 (GIS: Greenland Ice Sheet, AMOC: Atlantic Meridional Overturning Circulation, WAIS:
338 West Antarctic Ice Sheet, AMAZ: Amazon rainforest). This differential equation possesses
339 two different stable states: a baseline regime around $x_i \approx -1.0$ and a transitioned regime
340 around $x_i \approx +1.0$. $\Delta\text{GMT}(t)$ denotes the global mean surface temperature increase above
341 pre-industrial levels (as compared to the 1850–1900 level). This term is time dependent
342 because of the time dependence of the overshoot trajectory, which serves as our input:
343 $\Delta\text{GMT}(t) = \text{overshoot trajectory}(t)$. The mathematical form of the overshoot trajectory is
344 given below in the methods section: *temperature overshoot trajectories*. $T_{\text{crit},i}$ denotes the
345 critical temperatures for the four tipping elements. The interaction strength parameter is
346 indicated by d and is varied between 0.0 and 1.0, where $d = 0.0$ means no interaction between
347 the tipping elements and $d = 1.0$ means that interactions are approximately as important as the
348 individual dynamics. The link strength s_{ij} is taken from an expert elicitation²². Lastly, the time
349 scale-parameter τ_i denotes the tipping time of a particular tipping element. Of course, the four
350 stylised differential equations above (Eq. 1) are a strong simplification of the more complex
351 tipping elements. However, they represent a summary of the main stability patterns, as has
352 been argued in literature before^{23,42}. For more details on the mathematics in this model, please
353 be referred to Wunderling et al.(2021)²³.

354

355 **Parameter uncertainties.** There are uncertainties in several parameters of the model (see
356 Eq. 1 and supp. Tab. S1): (i) In the critical temperature regimes $T_{\text{crit},i}$, which are taken from the
357 recently refined literature values⁶. (ii) The interactions between the climate tipping elements
358 all represent physical mechanisms behind each pair of tipping elements. For instance a melting
359 Greenland Ice Sheet induces a freshwater input into the North Atlantic and, by that, weakens
360 the AMOC, while a weakening AMOC would reduce the warming over Greenland (see Fig. 1).
361 There is a considerable uncertainty of the link strength parameters s_{ij} , which are included in
362 our uncertainty analysis, and their values are taken from an expert elicitation on interacting
363 climate tipping elements²². The same values for interaction strengths have been used in earlier
364 research on tipping cascades²³. (iii) The upper and lower bounds for tipping times for the
365 four tipping elements are again taken from recent literature⁶. It is important to note that
366 the timescales for tipping vary from decades, over centuries up to millennia depending on
367 the respective tipping element. While the Amazon rainforest and the AMOC tip on shorter
368 timescales (decades to centuries), the Greenland and West Antarctic Ice Sheets take longer
369 to disintegrate (multiple centuries to millennia). These, on at least two orders of magnitude,
370 different tipping times have important effects on the dynamics of tipping, and as to whether a
371 specific tipping event occurs or not. These effects are discussed in the main text.

372

373 **Propagation of uncertainties via a Monte Carlo ensemble.** Since there are consider-
374 able uncertainties in the critical temperature regimes, interaction strengths and structure,
375 as well as in the tipping time scales, we set up a large-scale Monte Carlo ensemble to
376 adequately propagate the uncertainties in these parameters. The uncertainty range of the
377 parameter uncertainties are given in supp. Tab. S1. For each combination of peak tem-
378 perature ($T_{\text{Peak}} = 2.0, 2.5, \dots, 6.0^\circ\text{C}$), convergence temperature ($T_{\text{Conv}} = 0.0, 0.5, \dots, 2.0^\circ\text{C}$)
379 and convergence time ($t_{\text{Conv}} = 100, 200, \dots, 1000$ years), we draw 100 realisations from a

380 continuous uniform distribution using a latin hypercube algorithm⁴³ over the uncertainties
 381 in critical temperatures, link strengths and tipping times. These 100 realisations are looped
 382 over the 9 possible different network structures ([i] a positive link between WAIS→AMOC
 383 and a positive link between AMOC→AMAZ, [ii] a zero link between WAIS→AMOC and a
 384 positive link between AMOC→AMAZ, ..., [ix] a negative link between WAIS→AMOC and
 385 a negative link between AMOC→AMAZ). With this procedure, we obtain approximately 3.8
 386 million ensemble members in total. By drawing from a continuous uniform distribution for all
 387 tipping elements, we slightly overestimate the overall uncertainties and perform a maximum
 388 uncertainty assessment. Therefore, our errors are conservative. After 100 years, 1,000 years
 389 and in equilibrium (here: 50,000 years), we branch off the results for each of our 3.8 million
 390 ensemble members such that we can assess our results at these three different timings.

391

392 **Temperature overshoot trajectories.** In this study, we have used stylised temperature over-
 393 shoot trajectories based on overshoot trajectories that capture temperature profiles generated by
 394 Earth System Model simulations for a low to medium emissions scenario²⁴:

$$\Delta\text{GMT}(t) = T_0 + \gamma t - [1 - e^{-(\mu_0 + \mu_1 t)t}] [\gamma t - (T_{\text{Conv}} - T_0)]. \quad (2)$$

395 In this equation, the temperature overshoot trajectory $\Delta\text{GMT}(t)$ is determined via five
 396 parameters: (i) T_0 is the approximate current level of global warming, i.e. the point at which
 397 the trajectories start at $t = 0$. We have chosen $T_0 = 1.0^\circ\text{C}$ above pre-industrial levels. (ii)
 398 T_{Conv} is the final convergence temperature, for which we have chosen an ensemble approach
 399 comprising $T_{\text{Conv}} = 0.0, 0.5, 1.0, 1.5, 2.0^\circ\text{C}$ above pre-industrial. (iii) The parameter γ is
 400 chosen such that the global warming rate matches the recent past. The exponential decay term
 401 describes the development away from the linearly increasing trend (set by γ) bent towards the
 402 stabilisation level (set by T_{Conv}), specified by the parameters (iv) μ_0 and (v) μ_1 . In our ensemble,

403 we construct a temperature overshoot trajectory with a specific peak temperature T_{Peak} and
404 convergence time t_{Conv} by iteratively altering the parameters γ , μ_0 and μ_1 until it matches the
405 desired peak temperature and convergence time. Exemplary overshoot trajectories can be found
406 in supp. Fig. S1, where the chosen parameters correspond to Fig. 1a. The chosen parameter
407 values to get $T_{\text{Peak}} = 2.5^\circ\text{C}$ and $t_{\text{Conv}} = 400$ years are: $\gamma = 0.0963^\circ\text{C yr}^{-1}$, $\mu_0 = 1.5 \cdot 10^{-3} \text{ yr}^{-1}$,
408 and $\mu_1 = 1.83 \cdot 10^{-4} \text{ yr}^{-2}$. The convergence temperature is set to $T_{\text{Conv}} = 2.0^\circ\text{C}$. The
409 accuracy we require for our scenarios is $\Delta T_{\text{Peak}} < 0.025^\circ\text{C}$ and $\Delta t_{\text{Conv}} < 0.5$ years, where the
410 convergence time is determined as the time when the temperature overshoot curve has reached
411 the convergence temperature to an accuracy of 0.01°C .

412

413 **Notes on colour maps.** This paper makes use of perceptually uniform colour maps developed
414 by F. Crameri⁴⁴.

415

416 **Data and Code availability.** The data and code that support the findings of this study are avail-
417 able from the corresponding authors upon reasonable request. The python modelling package
418 *pycascades*, with which we simulated the dynamics of interacting tipping elements, is available
419 at <https://pypi.org/project/pycascades/>, together with a model description pa-
420 per⁴⁵. In case of questions or requests, please contact N.W..

References and Notes

- [1] Lenton, T. M. *et al.* Tipping elements in the Earth's climate system. *Proceedings of the National Academy of Sciences* **105**, 1786–1793 (2008).
- [2] Schellnhuber, H. J. Tipping elements in the earth system. *Proceedings of the National Academy of Sciences* **106**, 20561–20563 (2009).
- [3] Steffen, W. *et al.* Trajectories of the Earth System in the Anthropocene. *Proceedings of the National Academy of Sciences* **115**, 8252–8259 (2018).
- [4] Levermann, A. & Winkelmann, R. A simple equation for the melt elevation feedback of ice sheets. *The Cryosphere* **10**, 1799–1807 (2016).
- [5] Aragão, L. E. The rainforest's water pump. *Nature* **489**, 217–218 (2012).
- [6] Armstrong McKay, D. *et al.* Updated assessment suggests > 1.5°C global warming could trigger multiple climate tipping points (in review). *Earth and Space Science Open Archive* **80** (2021). URL <https://doi.org/10.1002/essoar.10509769.1>.
- [7] Schellnhuber, H. J., Rahmstorf, S. & Winkelmann, R. Why the right climate target was agreed in Paris. *Nature Climate Change* **6**, 649–653 (2016).
- [8] Garbe, J., Albrecht, T., Levermann, A., Donges, J. F. & Winkelmann, R. The hysteresis of the Antarctic ice sheet. *Nature* **585**, 538–544 (2020).
- [9] Robinson, A., Calov, R. & Ganopolski, A. Multistability and critical thresholds of the Greenland ice sheet. *Nature Climate Change* **2**, 429–432 (2012).
- [10] Hawkins, E. *et al.* Bistability of the Atlantic overturning circulation in a global climate model and links to ocean freshwater transport. *Geophysical Research Letters* **38** (2011).

- 442 [11] Nobre, C. A. & Borma, L. D. S. ‘Tipping points’ for the Amazon forest. *Current Opinion*
443 *in Environmental Sustainability* **1**, 28–36 (2009).
- 444 [12] Lenton, T. M. *et al.* Climate tipping points—too risky to bet against. *Nature* **575**, 592–595
445 (2019).
- 446 [13] Masson-Delmotte, V. P. *et al.* *IPCC, 2021: Climate Change 2021: The Physical Science*
447 *Basis. Contribution of Working Group I to the Sixth Assessment Report of the Intergovern-*
448 *mental Panel on Climate Change* (Cambridge University Press, 2021).
- 449 [14] Climate Analytics, NewClimate Institute, The Climate Action Tracker Ther-
450 mometer (2021). URL [https://climateactiontracker.org/global/](https://climateactiontracker.org/global/cat-thermometer/)
451 [cat-thermometer/](https://climateactiontracker.org/global/cat-thermometer/).
- 452 [15] Ritchie, P. D., Clarke, J. J., Cox, P. M. & Huntingford, C. Overshooting tipping point
453 thresholds in a changing climate. *Nature* **592**, 517–523 (2021).
- 454 [16] Tong, D. *et al.* Committed emissions from existing energy infrastructure jeopardize 1.5°C
455 climate target. *Nature* **572**, 373–377 (2019).
- 456 [17] Raftery, A. E., Zimmer, A., Frierson, D. M., Startz, R. & Liu, P. Less than 2°C warming
457 by 2100 unlikely. *Nature Climate Change* **7**, 637–641 (2017).
- 458 [18] Alkhayuon, H., Ashwin, P., Jackson, L. C., Quinn, C. & Wood, R. A. Basin bifurca-
459 tions, oscillatory instability and rate-induced thresholds for Atlantic Meridional Overturn-
460 ing Circulation in a global oceanic box model. *Proceedings of the Royal Society A* **475**,
461 20190051 (2019).
- 462 [19] Ritchie, P., Karabacak, Ö. & Sieber, J. Inverse-square law between time and amplitude for
463 crossing tipping thresholds. *Proceedings of the Royal Society A* **475**, 20180504 (2019).

- 464 [20] Rocha, J. C., Peterson, G., Bodin, Ö. & Levin, S. Cascading regime shifts within and
465 across scales. *Science* **362**, 1379–1383 (2018).
- 466 [21] Lenton, T. M. & Williams, H. T. On the origin of planetary-scale tipping points. *Trends*
467 *in Ecology & Evolution* **28**, 380–382 (2013).
- 468 [22] Kriegler, E., Hall, J. W., Held, H., Dawson, R. & Schellnhuber, H. J. Imprecise probability
469 assessment of tipping points in the climate system. *Proceedings of the National Academy*
470 *of Sciences* **106**, 5041–5046 (2009).
- 471 [23] Wunderling, N., Donges, J. F., Kurths, J. & Winkelmann, R. Interacting tipping elements
472 increase risk of climate domino effects under global warming. *Earth System Dynamics*
473 **12**, 601–619 (2021).
- 474 [24] Huntingford, C. *et al.* Flexible parameter-sparse global temperature time profiles that
475 stabilise at 1.5 and 2.0°C. *Earth System Dynamics* **8**, 617–626 (2017).
- 476 [25] Jones, C. D. *et al.* The Zero Emissions Commitment Model Intercomparison Project
477 (ZECMIP) contribution to C4MIP: quantifying committed climate changes following zero
478 carbon emissions. *Geoscientific Model Development* **12**, 4375–4385 (2019).
- 479 [26] MacDougall, A. H. *et al.* Is there warming in the pipeline? A multi-model analysis of the
480 Zero Emissions Commitment from CO₂. *Biogeosciences* **17**, 2987–3016 (2020).
- 481 [27] Williams, R. G., Roussenov, V., Frölicher, T. L. & Goodwin, P. Drivers of continued
482 surface warming after cessation of carbon emissions. *Geophysical Research Letters* **44**,
483 10–633 (2017).
- 484 [28] Zickfeld, K. *et al.* Long-term climate change commitment and reversibility: An EMIC
485 intercomparison. *Journal of Climate* **26**, 5782–5809 (2013).

- 486 [29] King, A. D. *et al.* Studying climate stabilization at Paris Agreement levels. *Nature Climate*
487 *Change* **11**, 1010–1013 (2021).
- 488 [30] Dekker, M. M., Von Der Heydt, A. S. & Dijkstra, H. A. Cascading transitions in the
489 climate system. *Earth System Dynamics* **9**, 1243–1260 (2018).
- 490 [31] Ciemer, C., Winkelmann, R., Kurths, J. & Boers, N. Impact of an AMOC weakening on
491 the stability of the southern Amazon rainforest. *The European Physical Journal Special*
492 *Topics* 1–9 (2021).
- 493 [32] Lohmann, J. & Ditlevsen, P. D. Risk of tipping the overturning circulation due to increas-
494 ing rates of ice melt. *Proceedings of the National Academy of Sciences* **118** (2021).
- 495 [33] Rietkerk, M. *et al.* Evasion of tipping in complex systems through spatial pattern forma-
496 tion. *Science* **374**, eabj0359 (2021).
- 497 [34] Drijfhout, S. *et al.* Catalogue of abrupt shifts in intergovernmental panel on climate change
498 climate models. *Proceedings of the National Academy of Sciences* **112**, E5777–E5786
499 (2015).
- 500 [35] Runge, J. *et al.* Identifying causal gateways and mediators in complex spatio-temporal
501 systems. *Nature Communications* **6**, 1–10 (2015).
- 502 [36] Irrgang, C. *et al.* Towards neural Earth system modelling by integrating artificial intelli-
503 gence in Earth system science. *Nature Machine Intelligence* **3**, 667–674 (2021).
- 504 [37] Drouet, L. *et al.* Net zero-emission pathways reduce the physical and economic risks of
505 climate change. *Nature Climate Change* **11**, 1070–1076 (2021).
- 506 [38] Riahi, K. *et al.* Cost and attainability of meeting stringent climate targets without over-
507 shoot. *Nature Climate Change* **11**, 1063–1069 (2021).

- 508 [39] Cai, Y., Lenton, T. M. & Lontzek, T. S. Risk of multiple interacting tipping points should
509 encourage rapid CO₂ emission reduction. *Nature Climate Change* **6**, 520–525 (2016).
- 510 [40] Cai, Y., Judd, K. L., Lenton, T. M., Lontzek, T. S. & Narita, D. Environmental tipping
511 points significantly affect the cost- benefit assessment of climate policies. *Proceedings of*
512 *the National Academy of Sciences* **112**, 4606–4611 (2015).
- 513 [41] Lemoine, D. & Traeger, C. P. Economics of tipping the climate dominoes. *Nature Climate*
514 *Change* **6**, 514–519 (2016).
- 515 [42] Bathiany, S. *et al.* Beyond bifurcation: using complex models to understand and predict
516 abrupt climate change. *Dynamics and Statistics of the Climate System* **1** (2016).
- 517 [43] Baudin, M. pyDOE: The experimental design package for python. URL [https://](https://pythonhosted.org/pyDOE/index.html)
518 pythonhosted.org/pyDOE/index.html.
- 519 [44] Cramer, F. Geodynamic diagnostics, scientific visualisation and staglab 3.0. *Geoscientific*
520 *Model Development* **11**, 2541–2562 (2018).
- 521 [45] Wunderling, N. *et al.* Modelling nonlinear dynamics of interacting tipping elements on
522 complex networks: the PyCascades package. *The European Physical Journal Special*
523 *Topics* 1–14 (2021).

524 **Acknowledgements**

525 This work has been carried out within the framework of PIK's FutureLab on Earth Resilience
526 in the Anthropocene. N.W., J.R., and J.F.D. acknowledge support from the European Research
527 Council Advanced Grant project ERA (Earth Resilience in the Anthropocene, ERC-2016-
528 ADG-743080). J.F.D. is grateful for financial support by the project CHANGES funded by the
529 Federal Ministry for Education and Research (BMBF) within the framework "PIK_Change"
530 under the grant 01LS2001A. R.W., J.R., D.I.A.M., S.L. and B.S. acknowledge financial support
531 via the Earth Commission, hosted by FutureEarth. The Earth Commission is the science
532 component of the Global Commons Alliance, a sponsored project of Rockefeller Philanthropy
533 Advisors, with support from Oak Foundation, MAVA, Porticus, Gordon and Betty Moore
534 Foundation, Herlin Foundation and the Global Environment Facility. The Earth Commission
535 is also supported by the Global Challenges Foundation. P.D.L.R. acknowledges support from
536 the European Research Council 'Emergent Constraints on Climate-Land feedbacks in the
537 Earth System (ECCLES)' project, grant agreement number 742472. The authors gratefully
538 acknowledge the European Regional Development Fund (ERDF), the BMBF and the Land
539 Brandenburg for supporting this project by providing resources on the high performance
540 computer system at the Potsdam Institute for Climate Impact Research.

541

542 **Author contributions**

543 R.W., J.R. and J.F.D. conceived the study. N.W. designed the study, performed the simulations
544 and led the writing of the manuscript with input from all authors. N.W., S.L. and B.S. prepared
545 the figures with input from R.W., J.R. and J.F.D.. J.F.D. led the supervision of this study.

546

547 **Additional information**

548 Supplementary information is available in the online version of the paper. Reprints and per-

549 missions information are available online at www.nature.com/reprints. Requests for materials
550 should be addressed to N.W.

551

552 **Competing interests**

553 The authors declare no competing interests.

Supplementary Files

This is a list of supplementary files associated with this preprint. Click to download.

- [supplement.pdf](#)